Hindawi Publishing Corporation
Journal of Nanoparticles
Volume 2015, Article ID 601941, 9 pages
http://dx.doi.org/10.1155/2015/601941

Research Article

Structured Pd/γ-Al_2O_3 Prepared by Washcoated Deposition on a Ceramic Honeycomb for Compressed Natural Gas Applications

Małgorzata Adamowska and Patrick Da Costa

Institut Jean le Rond d'Alembert, Université Pierre et Marie, Curie (UPMC Paris 6), CNRS UMR 7190, 2 Place de la Gare de Ceinture, 78210 Saint Cyr l'Ecole, France

Correspondence should be addressed to Małgorzata Adamowska; malgorzata.adamowska@wp.pl

Received 27 July 2014; Accepted 30 September 2014

Academic Editor: Amir Kajbafvala

The preparation of a coating procedure was studied, from the washcoating with γ-alumina to the deposition of palladium by excess solvent or incipient wetness impregnation. The powder and the washcoat layers were studied by different characterisation techniques such as SEM, BET surface area, and XRD. Vibration-resistance and heat-resistance were also evaluated. It was shown that the alumina layer is quite well deposited on the channel walls (SEM images). However, a detachment of the washcoat layer was observed after ultrasound treatment. It was proved that the monolith Pd impregnation method by incipient wetness impregnation is more efficient. The presence of palladium was confirmed using HRTEM, the palladium was present under the Pd (II) oxidation state, and the size of PdO particles varies between 2.5 and 3.1 nm. The catalytic properties of the monolith catalyst were carried out using temperature programmed surface reaction (TPSR). The efficiency of the procedure of the monolith catalyst preparation was confirmed by comparing the activity of the prepared catalyst with the one of a model catalyst.

1. Introduction

Automobile exhaust constitutes an important source of air pollution. The compounds emitted in the exhaust can be divided into two categories: those that are regulated by law, that is, carbon monoxide (CO), nitrogen oxides (NOx), hydrocarbons (HC), and particulate, and unregulated constituents. The pollutant emissions from road vehicles are regulated separately for light-duty vehicles (cars and light vans) and for heavy-duty vehicles (trucks and buses). European emission standards such as Euro 6 (2014), Euro 6.2 (2017), and Euro 7 (2018) define the acceptable limits for exhaust emissions of new vehicles sold in EU member states [1, 2].

Natural gas (NG) is a favorable alternative automotive fuel due to its availability, low price, high hydrogen to carbon ratio, and lower CO_2 emission compared to conventional fuelled vehicles. However, a major disadvantage of using natural gas is the unburned CH_4 emission (effective greenhouse gas). Therefore, to comply with future legislation, highly efficient catalysts for the complete abatement of the unburned methane are needed [3]. Such catalysts are mainly composed by palladium deposited on typical supports [4].

For such an application in stoechiometric conditions, the use of three-way catalytic converters to minimise air pollution caused by automotive exhaust gases is already well established [5–7] for vehicles fuelled by gasoline. The typical three-way catalysts (TWC) contain noble metals (Pt, Pd, and Rh) deposited together with a washcoat (alumina modified with low loadings of lanthanum or barium and with ca. 10–20 wt.% ceria and zirconia) on a ceramic or metallic monolith [5]. The air/fuel (A/F) ratio is controlled within a narrow operating window, in which both the oxidation of hydrocarbons and carbon monoxide and the reduction of nitrogen oxides are promoted [8, 9]. However, only few studies deal with the use of catalysts used in simulated exhaust gases from CNG (compressed natural gas) vehicles [4, 10–12].

The monolith parts themselves can be produced in a number of sizes and shapes, typically round or oval cross-sectional areas for automotive applications, or square for stationary emission uses [13]. The number of channels, their

diameters, and wall thickness determine the cell density, expressed as cells per square inch (cpsi), which in turn allows the calculation of the geometric surface area which is the sum of the areas of all the channel walls upon which the catalyst is deposited [14].

The most common material for monolithic structures is cordierite, a ceramic material consisting of magnesia, silica, and alumina in the molar ratio of 2 : 5 : 2. Ceramic materials such as cordierite have high mechanical resistance, high melting temperatures (1465°C), and resistance to oxidation and can be made to have excellent thermal shock resistance (low expansion coefficients: $\leq 5 \times 10^{-6}\ K^{-1}$) [14–17]. Nevertheless, the monolithic ceramic catalyst has a low specific surface area (typically $0.7\ g{\cdot}m^{-2}$). This is the reason why a layer of oxide material with a high surface area (e.g., for γ-alumina, typically $200\ g{\cdot}m^{-2}$), called washcoat, is generally coated on the inner walls of the honeycomb support. The slurry coating of different materials was discussed by Addiego et al. [18]. Moreover, the preparation of monolithic catalysts has been reviewed in detail by Nijhuis et al. [19]. Alumina is always chosen because of its high surface area and relatively good thermal stability under hydrothermal conditions of the exhausts. However, it should be noted that γ-alumina can be transformed to α-alumina at high temperature (above 1000°C) which can be encountered in the three-way catalysis. Recrystallization to α-alumina leads to sintering and consequently to a severe drop of the surface area ($10\ g{\cdot}m^{-2}$) [20]. So the γ-alumina should be thermally stabilized by addition of stabilising agents such as lanthanum, barium, strontium, cerium, and, more recently, zirconium oxides [21, 22].

The washcoat is usually applied by impregnation of the honeycomb in slurry of the powder and subsequent drying and calcination. The last step is very important since the calcination binds the washcoat to the monolith walls and is usually done at temperatures of 550°C or higher [15].

The quality of the deposited washcoat depends on the slurry properties such as properties of the solid particles (nature and particle size) [23], properties of the solvent (nature and concentration) [24], and the amount of solids in the slurry [25].

An active element can be incorporated into the layer either during the washcoating step or after the washcoat step, using well-known techniques (wet impregnation, ion exchange, or deposition-precipitation) [19, 26].

In the present work, we first developed a simple procedure leading to a reproducible alumina washcoat. Secondly, we elaborated a procedure of Pd/Al_2O_3/cordierite monoliths preparation. We started our studies using only a Pd active phase to confirm the procedure efficiency by comparing the activity of our catalyst with the one of a model catalyst. The main objective of our work is to develop a new catalyst for natural gas vehicle (GNV) applications which will be more durable (activity stabilisation) and less expensive. So this procedure will be able to design and prepare any catalyst in the laboratory scale in the future. The thermal resistance studies of the new catalyst composition which corresponds to the different ageing processes will be also one of the objectives of our future work. The preliminary studies on the effects of thermal ageing on the structural and textural evolution of γ-alumina and the first correlation between the thermal ageing and a mathematical model have already been published [27].

2. Materials and Methods

2.1. Simple Washcoating Procedure. A commercial monolithic cordierite provided by Corning with a cell density of 400 cpsi was used as the support. The boehmite γ-AlOOH (SASOL DISPAL 23N4-80) was chosen as starting material for the washcoat preparation. The γ-alumina was obtained by the dehydration of γ-AlOOH during calcination. The powder of the starting material was milled to obtain particles of similar size as the macropores in the cordierite and then mixed with the necessary amount of binding agent (20 wt.% of colloidal alumina) and demineralised water in order to prepare the slurry. The slurry stabilization was obtained by nitric acid addition (68 wt.%). This step is not easy because of the complex influence of the acid concentration on the gelation process. Two different processes, namely, surface charging and dissolution, can take place [28].

The monoliths (37 mm length, 23 mm diameter) were dipped vertically into the slurry for 2 minutes. The excess of slurry was shaken out of the monolith and the blocked channels were cleared using pressurized air. Then the monolith was dried horizontally in air while being continuously rotated around its axis. Finally, the monolith was dried at 110°C for 2 hours and calcined at 550°C for 4 hours. This high temperature calcination step permitted to fix the coating to the monolith walls. The monolith was coated again before the calcination step using the same slurry composition. The washcoat loading was determined by weighting.

2.2. Procedure of Monolith Pd Impregnation. The palladium (1 wt.% referred to as the washcoat layer) was incorporated into the layer either by excess solvent impregnation or by incipient wetness impregnation.

In the first case, the aluminium washcoated monolith was dipped into the palladium solution. The impregnation was carried out using an evaporator (60°C, 180 rotations per minute). The wet impregnated monoliths were dried at 110°C for 2 hours and calcined at 550°C for 4 hours in air with a heating rate of $10°C{\cdot}min^{-1}$.

In the second case, the monolith was dipped into the Pd catalyst slurry always using the same washcoating procedure in Section 2.1. Supported Pd catalyst, prepared by incipient wetness impregnation, was employed as starting material for the washcoat preparation. The Pd catalyst precursor was dried at 110°C for 2 hours and calcined at 550°C for 4 hours in air with temperature ramp of $10°C{\cdot}min^{-1}$.

In both cases, an aqueous solution of tetramine palladium nitrate solution ($Pd(NH_3)_4(NO_3)_2$) was used as palladium precursor.

2.3. Physicochemical Characterizations. The powder X-ray diffraction patterns were recorded with a SIEMENS D500 diffractometer using monochromatised CuKα radiation.

Measurements were carried out for 2θ ranging from 10° up to 70°.

The specific surface areas were measured by nitrogen adsorption at −196°C using the multipoint method (Micromeritics ASAP 2010). The samples were previously treated at 110°C under vacuum (2×10^{-3} torr) for 3 hours.

The starting material was milled using a planetary micro mill Pulverisette 7 and the particle size distributions of milled powder were measured by a laser particle size analyzer (ANALYSETTE 22-COMPACT) with a measurement range from 0.3 to 300 μm. The analysis of the scattered light information in the analysette 22 was based on Fraunhofer or Mie theory. A volume distribution based on the equivalent diameter of the laser diffraction was obtained.

The washcoat quality of the coated honeycombs was studied by a JEOL JSM-5510 LV scanning electron microscope (SEM) equipped for EDS (energy dispersive spectroscopy) analysis. SEM images of the alumina washcoats were obtained on pieces cut from monolith after metallization of theses samples under an Au film.

The Pd species were studied by HRTEM on a JEOL-JEM 2011 HR (LaB) device equipped for EDS analysis. During the same analyses, EDS measurements were performed to verify the presence of palladium in the analyzed zone. The interplanar spacing was measured directly on the HRTEM images. The identification of Pd species was realized using JCPDS patterns [29].

Resistance to mechanical vibrations was evaluated using ultrasonic vibrations. A piece of the prepared monolith was treated in an ultrasound water bath (power 220 W, frequency 35 kHz). Finally the sample was dried and weighted. The adhesion properties between the catalyst and ceramic surface were determined by weight loss of the monolith as a function of time. The weight loss of sample after ultrasonic vibration was defined as follows:

$$\Delta W = \left[\frac{(W_1 - W_2)}{W_1}\right] \times 100\%, \quad (1)$$

where W_1 is the washcoat weight before ultrasonic vibration and W_2 is the washcoat weight after ultrasonic vibration.

Resistance to high temperature was studied using a piece of the loaded monolith in order to simulate an ageing process. This ageing process was performed in an oven at 950°C for 4 hours with a heating rate of 10°C·min^{-1} using 10 vol.% of water in air. These conditions correspond to the cracking and detaching state of a layer after using a vehicle for 50000 km.

2.4. Catalytic Activity Tests. The evaluation of the catalytic performance was carried out using temperature programmed surface reaction (TPSR). The TPSR was performed from room temperature (RT) to 570°C with a heating rate of 10°C·min^{-1} using the following gas mixture: 2500 ppm NO, 1700 ppm CH_4, 4800 ppm O_2, 4700 ppm CO, 3400 ppm H_2, 9.25% CO_2, and 18% H_2O which is representative of a real CNG exhaust gases mixture. This composition corresponds to a richness of 1.0005. The hour space velocity (GHSV) was 40,000 h^{-1}.

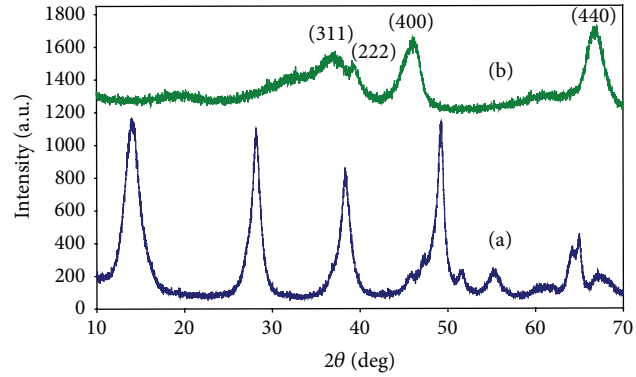

Figure 1: XRD powder patterns of samples: (a) pseudoboehmite and (b) γ-alumina.

To be close to industrial conditions, our apparatus showed a preheater in which the gases are heated up to 790°C. These heated gases flowed through the catalytic bed composed by the monolith sample. Three thermocouples were available to follow the reaction temperature. The first one was placed prior to the catalyst, the second one close to the catalyst, and the third one at the exit of the reactor.

The reactor outflow was analyzed using a set of specific detectors. An Eco Physics NO_x L Chemiluminescence's analyzer (for NO and total NO_x) allowed the simultaneous detection of both NO, NO_2 and NO_x (0–2500 ppm). An IR analyser was used to monitor N_2O and CH_4 (0–2500 ppm). The CO was analyzed by two specific IR analyzers dedicated to low (0–2000 ppm) and high CO concentrations (1–5%). The CO_2 was monitored by Rosemount analytical detector (0–20%).

3. Results and Discussion

3.1. Characterization of Starting Material. The γ-alumina was obtained by the γ-AlOOH dehydration during calcination step. The temperatures at which these transitions have been observed are somewhat variable, apparently dependent on the crystallinity and previous history of the boehmite and on the conditions of heat treatment [30, 31].

The dehydration of γ-AlOOH to γ-Al_2O_3 was realized at 500°C for 4 hours. The XRD patterns of the boehmite and γ-alumina are presented in Figure 1. Some of the peaks of the boehmite sample are broad and well defined (14.3°, 28.3°, 38.5°, 49.3°, and 55.5°). The broad diffraction lines of the boehmite reveal that the crystallites are very small. The boehmite structure corresponds to an orthorhombic unit cell. The boehmite sample was classified as a pseudoboehmite since the peaks are not sharp and intense [32].

The diffraction peaks of the calcined sample (37.3°, 39.6°, 46.2°, and 67°) can be indexed to a face-centered cubic phase of γ-Al_2O_3 (JSPDS n° 00-010-0425). We can observe a decrease of the peak intensity and the appearance of the main peaks characteristic of γ-alumina after pseudoboehmite calcination.

The specific surface area, total pore volume, and mean pore diameter results of the samples are reported in Table 1.

Table 1: BET surface area, total pore volume, and mean pore diameter of the pseudoboehmite and γ-Al_2O_3 (fresh and aged).

Sample	S_{BET} [$m^2 \cdot g^{-1}$]	Total pore volume [$cm^3 \cdot g^{-1}$]	Mean pore diameter [nm]
γ-AlOOH	293	0,35	4,6
γ-Al_2O_3	201	0,42	8,4
γ-Al_2O_3 aged	115	0,43	14,9

Recrystallization to γ-alumina leads to sintering and consequently to a severe drop of boehmite specific surface area. Average pore diameter ranges from 4.6 nm for the boehmite to 8.4 nm for the γ-alumina. Thus, according to the IUPAC classification, the starting materials studied show mesoporosity.

The specific surface area considerably decreased after the hydrothermal ageing process. This phenomenon is explained by water vapour presence which not only accelerates crystallization but also causes structural change in the oxide support [33].

3.2. Washcoating of Cordierite Monolith

3.2.1. γ-Al_2O_3 Coating. The washcoated monolith contains 23 wt.% (134 $g \cdot L^{-1}$) of the alumina layer after two impregnations.

The SEM images (Figures 2(a)-2(b)) of the washcoated monolith, obtained by secondary electrons detection (SEM-SEI images), show that the alumina layer is well deposited on the channel walls and the washcoat is observed in all the corners. However, we can also observe cracks in the coat layer. The cracks in the corners of the channels can be formed most likely because of a difference in thermal expansion between the cordierite and the alumina, while the cracks in the coat layer can be formed during a too fast drying step. Forzatti et al. [34] indicate that the drying step requires a careful control of temperature and moisture and the steps must be slow enough to prevent ruptures and cracks. It is evident that the problem of an inhomogeneous moisture distribution during drying step must be solved in the future studies.

The thickness of the alumina washcoat varies from 25 μm in the middle of the channels up to 85 μm in the corners (Figure 2(b)). The results obtained showed that the washcoat layer is well deposited over the whole channels length. However, the layer thickness is not homogeneous since the chemical elements distribution studied by EDS cartography is not uniform (results not shown). As it was mentioned previously, the main components of the cordierite are Al, Si, and Mg. Some silicon, which is not an element of the washcoat composition, was detected in the middle of some channels suggesting that the layer thickness is less important.

Thermal and mechanical treatments were realized to determine the initial resistance of the prepared catalyst. This information is necessary to develop more resistant catalytic material in the future. Resistance to mechanical vibrations and resistance to high temperature of the alumina washcoat were determined to simulate the conditions occurring in vehicles. The severe conditions (hot exhaust gases of high velocity and mechanical vibrations) can lead to detachment of the washcoat layer. Therefore, the adhesion of the substrate is a very important requirement. This study was carried out for samples before (fresh catalyst) and after ageing process (ageing catalyst). The weight loss curves of the washcoat are shown in Figure 3.

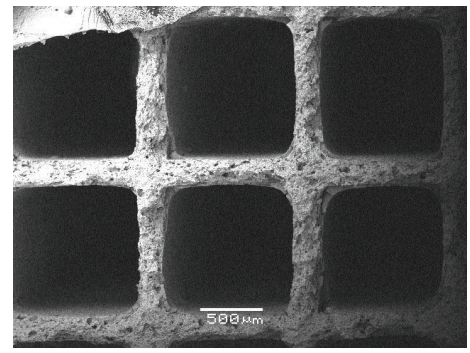

(a)

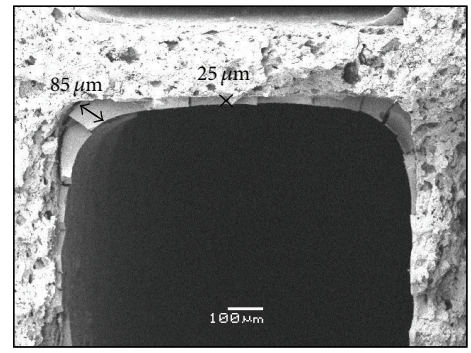

(b)

Figure 2: SEM images of the γ-Al_2O_3 washcoat layer on the cordierite monolith: (a) general view of the monolith piece and (b) view of one channel.

It can be observed that the washcoat exhibits a weight loss in both cases. However, this phenomenon is more significant for the sample exposed to a high temperature treatment. In the case of the fresh catalyst, the washcoat stabilisation is achieved after 2 hours of ultrasound treatment (the total weight loss around 9 wt.%). However, the layer stabilisation of ageing catalyst is observed after 15 hours (the total weight loss around 20 wt.%).

The cracks formation and propagation, as a result of the thermal stress during the drying and the high temperature treatments, have an influence directly on the washcoat detachment [35]. The numerical analysis of the wet body deformation by drying (an increase of the cohesive force, decohesion of the structure) was studied in detail by Kowalski et al. [36, 37].

The present works only show the elaboration of a simple washcoat procedure. However, it will be interesting in the future to modify the γ-alumina coating (Ce, Zr, La, or Ba addition) to improve the washcoat properties toward the thermal stress [20, 25].

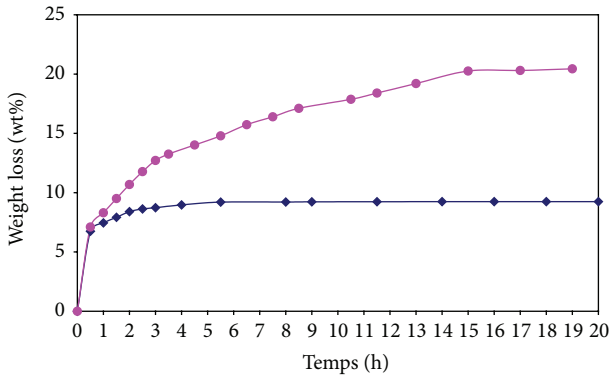

FIGURE 3: Weight loss of washcoat, as function of time (◆: before ageing, ●: after ageing).

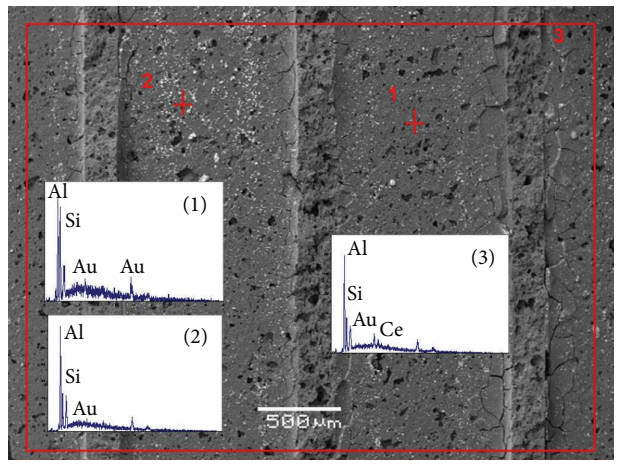

FIGURE 4: Internal surface studies of Pd-impregnated coating (Pd deposited by excess solvent impregnation) by EDS analysis.

3.2.2. Pd Catalyst Coating. The excess solvent impregnation and incipient wetness impregnationwere used to prepare the Pd-impregnated monoliths.

Excess Solvent Impregnation. The alumina washcoated quality was determined by SEM. The results show that the alumina layer is well deposited on the channel walls (results not shown). The efficiency of the Pd impregnation method was determined by EDS analysis.

The different zones were studied to obtain more precise information on the Pd distribution. Figure 4, one of the recorded spectra on the sample surface (different areas), shows the chemical elements present on the channel walls. Only aluminium, silicon, and gold peaks were observed during the EDS analysis. The Pd presence was not confirmed in the analysis zones. It was found that the majority of the palladium was deposited on the external surface of the impregnated monolith (Figure 5). It was concluded that the Pd impregnation of monolith method by excess solvent impregnation is unsuitable.

Incipient Wetness Impregnation. The washcoat quality was determined by SEM. SEM-SEI images (Figure 6) show that the cordierite support is completely covered. The thickness of the alumina washcoat varies from 21 μm in the middle of channel up to 72 μm in the corners. The EDS analysis (Figure 6) confirmed palladium presence on the channel walls. We can conclude that the method of palladium impregnation is efficient. The distribution of the Al and Si elements on the sample surface was determined by cartographies. Figure 6(a) shows that the washcoat layer is well deposited on the external parts of the monolith sample. The presence of silicon in the middle of the channel in the case of the internal part of the monolith sample (Figure 6(b)) indicates that the layer thickness is not homogeneous.

The Pd species was determined by HRTEM (Figure 7). The presence of palladium in each analyzed area was confirmed by EDS analysis. The lattice fringes were measured directly on the image using high magnifications view. The palladium species were then identified using a database of powder diffraction patterns. The results show that palladium is present under the PdO oxidation state and the size of these particles varies between 2.5 and 3.1 nm.

3.3. Catalytic Activity Tests. The commercial honeycomb converter is mainly composed by the palladium oxide (2.55 wt.%) and a small amount of rhodium (0.18 wt.%) and platinum (0.07 wt.%) [4]. Salaün et al. [4] concluded that the palladium is deposited on the alumina whereas rhodium is deposed on the ceria-zirconia.

For CNG applications, methane, which is the major component of natural gas, is the main pollutant. The palladium in PdO form is presented as the more active phase for methane oxidation [4]. In order to evaluate the performance of the washcoating procedure, we prepared a catalyst containing 2.5 wt.% of palladium to compare its activity with a model catalyst which contains the same amount of palladium provided by an international catalyst manufacturer.

In Figure 8, NO_x, CH_4, and CO conversions are reported as a function of the reaction temperature for the prepared (a) and the model (b) Pd monolith catalysts. At low temperatures, we observe the evolution of the NO_x concentration which is correlated to the N_2O formation. This phenomenon is observed for both catalysts; however, the amount of N_2O formed is more important in the case of the model catalyst.

According to the literature [4, 11], at low temperature, NO can be reduced by hydrogen or carbon monoxide, whereas at high temperature the methane is the reducing agent of NO. Salaün et al. [11] investigated the role of CO and H_2 in NO reduction removing the hydrogen or the oxygen from the feed. In absence of H_2, the NO conversion was decreased significantly and the light off temperature was shifted to higher temperature. In absence of CO, the global trends of the plots of NO reduction and CH_4 oxidation were comparable with those obtained for the total gas mixture. These authors showed that the major reducing agent for NO reduction at low temperature is hydrogen.

At low temperature, we can also observe the carbon monoxide conversion which is oxidized by oxygen (Figure 8). Salaün et al. [4] proposed that the CO oxidation and the

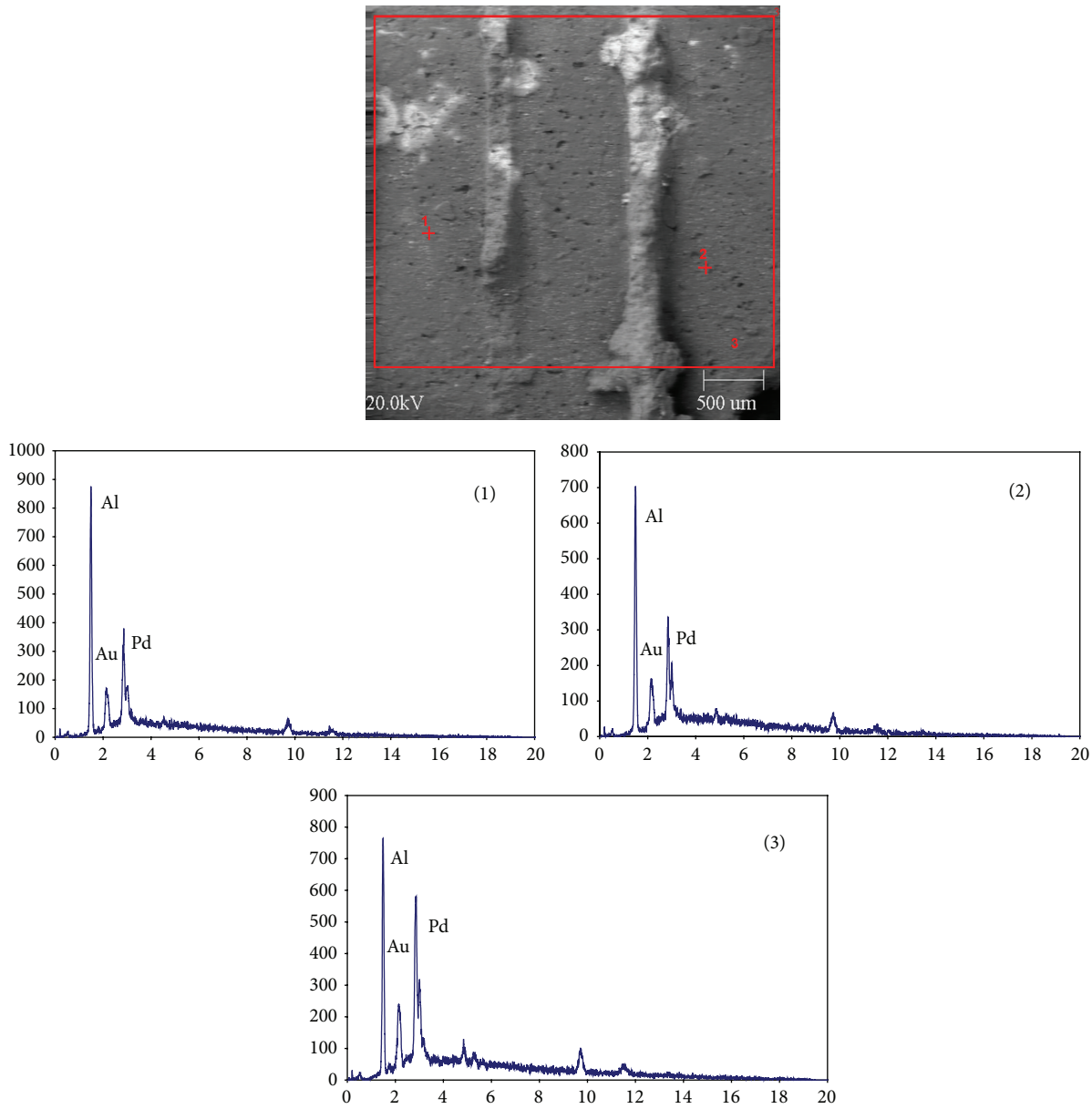

Figure 5: External surface studies of Pd-impregnated coating (Pd deposited by excess solvent impregnation) by EDS analysis.

NO reduction do not take place on the same catalytic site (rhodium and palladium sites, respectively). Furthermore, these authors supposed that a reaction between CO and N_2O (product of NO decomposition or reduction at low temperature) is possible since less N_2O quantity is detected. However, at high temperature, CO could be consumed during the water gas shift reaction. We observed that in the case of the prepared catalyst, the light off temperature is shifted to lower temperature.

At high temperature, we can also observe simultaneously NO_x and CH_4 conversion. The methane is completely converted below 560°C. Salaün et al. [4] showed that the main oxidizing agent of methane is NO. However, these authors suggest that, at high temperature, the steam effects are not negligible. We can observe that the evolution of the methane concentration was the same for model and prepared catalysts. The results obtained show that our catalyst is as good as the model catalyst and that the procedure of our monolith preparation is efficient.

The prepared catalyst is active in the methane oxidation reaction. However, it is evident that its composition must be optimised to reinforce its catalytic action and to stabilise the alumina transformation.

4. Conclusions

The washcoat layer is well deposited on the channel walls and in the corners. However, the layer thickness is not homogeneous. The cracks observed on the coat layer and in the corners of the channels were formed most likely because

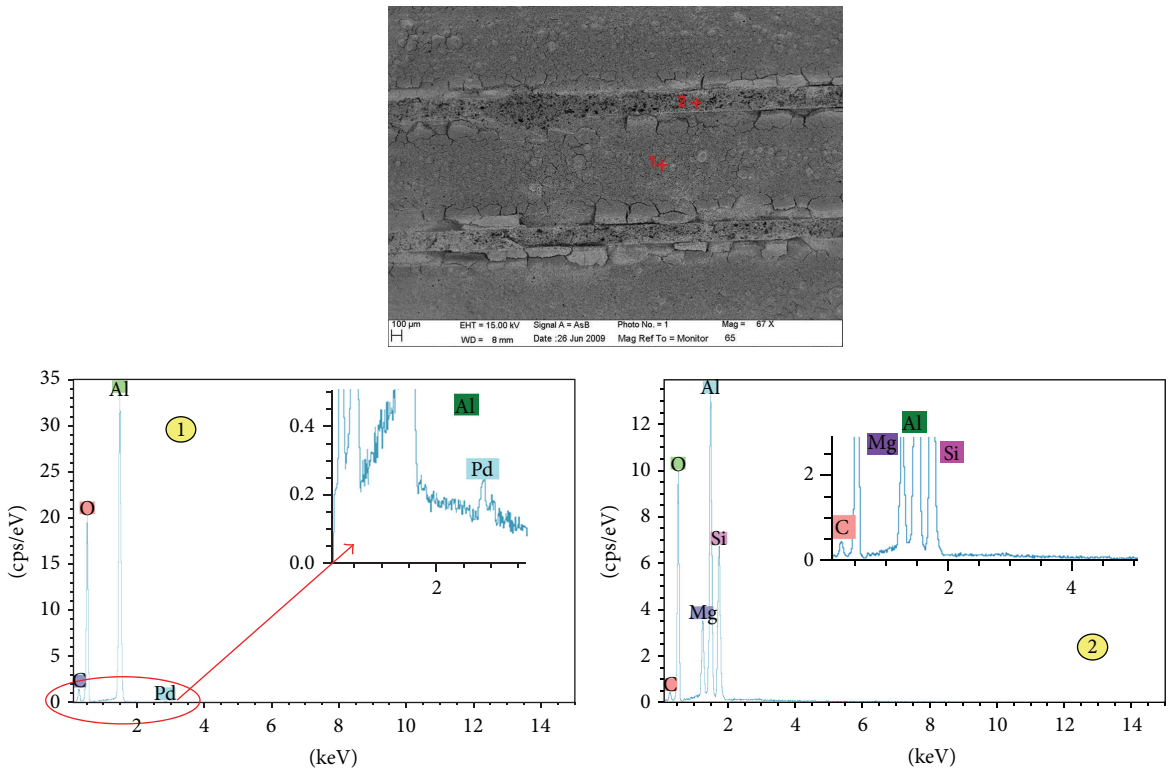

FIGURE 6: EDS analysis of Pd-impregnated coating (Pd deposited by incipient wetness impregnation).

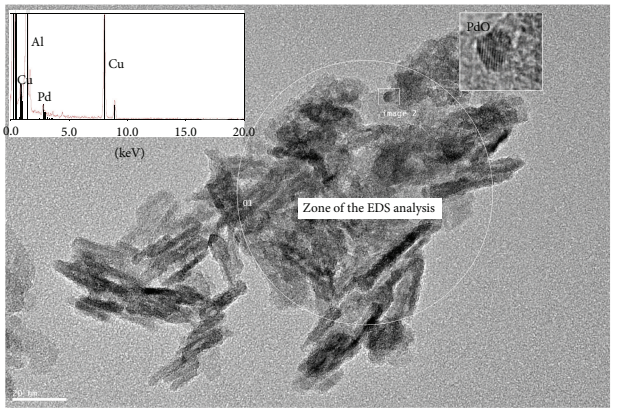

FIGURE 7: Transition electron microscopy of Pd-impregnated monoliths, coupled with EDS spectroscopy.

of a difference in thermal expansion and during a too fast drying step. Obviously, the drying step (temperature and moisture control) has to be optimized.

A detachment of the washcoat layer was observed after ultrasound treatment for fresh and aged catalysts. However, this phenomenon is more significant for the sample exposed to a high temperature treatment. The washcoating procedure must be optimized to increase the coating adhesion.

The Pd impregnation of monolith by incipient wetness impregnation is more efficient than the excess solvent impregnation method. The Pd is present under the Pd (II) oxidation state.

The prepared catalyst is active in the methane oxidation reaction. The results obtained show that our catalyst is as good as the model catalyst and that the procedure of our monolith preparation is efficient.

The main goal of our research is to develop a new catalyst for GNV applications. The know-how of the washcoating procedure allows us to optimize the catalyst composition, such as the active phase and the stabilizing agent of alumina. The objective is to improve the catalytic performance and to decrease the price of the catalyst. This monolithic catalyst will be also applied for the methane oxidation and the selective catalytic reduction of NO_x by methane.

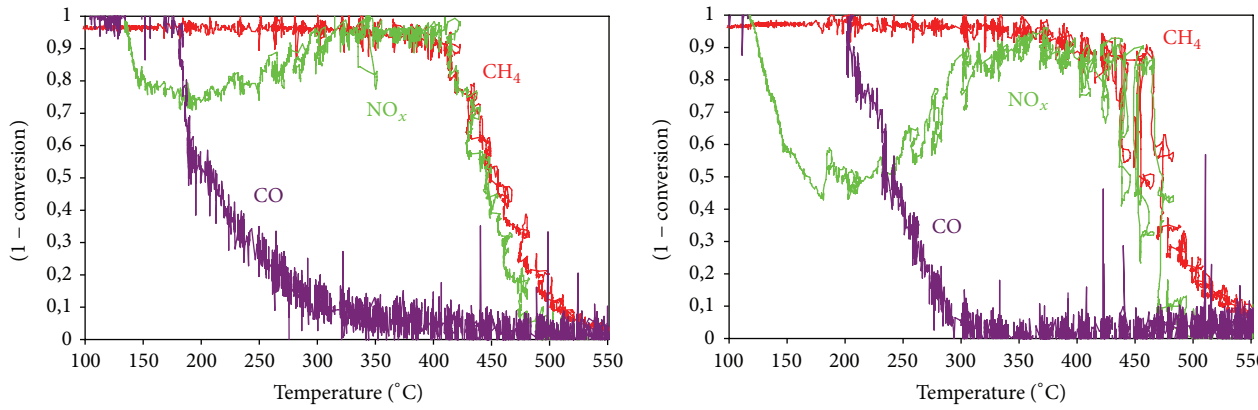

FIGURE 8: TPSR profile of NO_x, CH_4, and CO for (a) prepared catalyst and (b) model catalyst. Feed gas: 2500 ppm NO, 1700 ppm CH_4, 4800 ppm O_2, 4700 ppm CO, 3400 ppm H_2, 9.25% CO_2, and 18% H_2O and balance N_2 (GHSV 40,000 h^{-1}).

Conflict of Interests

The authors declare that there is no conflict of interests regarding the publication of this paper.

Acknowledgments

This study was carried out in the framework of ANR CARAVELLE. The authors are grateful to ADEME for the financial support and Mrs. Sandra Casale and M. Stéphane Borenstein for TEM and SEM studies.

References

[1] P. Bielaczyc, J. Woodburn, and A. Szczotka, "An assessment of regulated emissions and CO_2 emissions from a European light-duty CNG-fueled vehicle in the context of Euro 6 emissions regulations," *Applied Energy*, vol. 117, pp. 134–141, 2014.

[2] G. A. Rhys-Tyler, W. Legassick, and M. C. Bell, "The significance of vehicle emissions standards for levels of exhaust pollution from light vehicles in an urban area," *Atmospheric Environment*, vol. 45, no. 19, pp. 3286–3293, 2011.

[3] A. M. Venezia, G. di Carlo, G. Pantaleo, L. F. Liotta, G. Melaet, and N. Kruse, "Oxidation of CH_4 over Pd supported on TiO_2-doped SiO_2: effect of Ti(IV) loading and influence of SO_2," *Applied Catalysis B: Environmental*, vol. 88, no. 3-4, pp. 430–437, 2009.

[4] M. Salaün, A. Kouakou, S. da Costa, and P. da Costa, "Synthetic gas bench study of a natural gas vehicle commercial catalyst in monolithic form: on the effect of gas composition," *Applied Catalysis B: Environmental*, vol. 88, no. 3-4, pp. 386–397, 2009.

[5] J. K. Hochmuth, K. Wassermann, and R. J. Farrauto, "Car exhaust cleaning," in *Reference Module in Chemistry, Molecular Sciences and Chemical Engineering*, vol. 7 of *Comprehensive Inorganic Chemistry*, pp. 505–523, 2013.

[6] K. A. Subramanian, V. C. Mathad, V. K. Vijay, and P. M. V. Subbarao, "Comparative evaluation of emission and fuel economy of an automotive spark ignition vehicle fuelled with methane enriched biogas and CNG using chassis dynamometer," *Applied Energy*, vol. 105, pp. 17–29, 2013.

[7] G. Karavalakis, M. Hajbabaei, T. D. Durbin, K. C. Johnson, Z. Zheng, and W. J. Miller, "The effect of natural gas composition on the regulated emissions, gaseous toxic pollutants, and ultrafine particle number emissions from a refuse hauler vehicle," *Energy*, vol. 50, no. 1, pp. 280–291, 2013.

[8] M. Shelef and H. S. Gandhi, "Ammonia formation in catalytic reduction of nitric oxide by molecular hydrogen: II. Noble metal catalysts," *Industrial & Engineering Chemistry Product Research and Development*, vol. 11, no. 4, pp. 393–396, 1972.

[9] Y.-F. Y. Yao, "The oxidation of CO and hydrocarbons over noble metal catalysts," *Journal of Catalysis*, vol. 87, no. 1, pp. 152–162, 1984.

[10] P. da Costa, M. Salaün, G. Djéga-Mariadassou, S. da Costa, and G. Brecq, "Comparative study of natural gas vehicles commercial catalysts in monolithic form," SAE Technical Paper 2007-01-0039, 2007.

[11] M. Salaün, S. Capela, S. Da Costa, L. Gagnepain, and P. Da Costa, "Enhancement of 3-way CNG catalyst performance at high temperature due to the presence of water in the feed: on the role of steam reforming of methane and on the influence of ageing," *Topics in Catalysis*, vol. 52, no. 13–20, pp. 1972–1976, 2009.

[12] M. Adamowska, V. Lauga, and P. da Costa, "Elaboration of an accelerated oven CNG heavy duty vehicles catalyst ageing for road ageing simulation," *Topics in Catalysis*, vol. 56, no. 1–8, pp. 267–272, 2013.

[13] J. L. Williams, "Monolith structures, materials, properties and uses," *Catalysis Today*, vol. 69, no. 1–4, pp. 3–9, 2001.

[14] R. M. Heck, S. Gulati, and R. J. Farrauto, "The application of monoliths for gas phase catalytic reactions," *Chemical Engineering Journal*, vol. 82, no. 1–3, pp. 149–156, 2001.

[15] A. Pedro, M. Montes, and E. E. Miró, "Monolithic reactors for environmental applications: a review on preparation technologies," *Chemical Engineering Journal*, vol. 109, no. 1, pp. 11–36, 2005.

[16] M. Valáškováa, J. Zdrálkováa, J. Tokarskýa, G. Simha Martynkováa, M. Ritzc, and S. Študentová, "Structural characteristics of cordierite/steatite ceramics sintered from mixtures containing pore-forming organovermiculite," *Ceramics International*, vol. 40, pp. 15717–15725, 2014.

[17] T. Zhou, L. Li, J. Cheng, and Z. Hao, "Preparation of binary washcoat deposited on cordierite substrate for catalytic applications," *Ceramics International*, vol. 36, no. 2, pp. 529–534, 2010.

[18] W. P. Addiego, I. M. Lachman, M. D. Patil, J. L. Williams, and K. E. Zaun, "High surface area washcoated substrate and method for producing same," US Patent 5,212,130, 1993.

[19] T. A. Nijhuis, A. E. W. Beers, T. Vergunst, I. Hoek, F. Kapteijn, and J. A. Moulijn, "Preparation of monolithic catalysts," *Catalysis Reviews: Science and Engineering*, vol. 43, no. 4, pp. 345–380, 2001.

[20] J. Kašpar, P. Fornasiero, and N. Hickey, "Automotive catalytic converters: current status and some perspectives," *Catalysis Today*, vol. 77, no. 4, pp. 419–449, 2003.

[21] P. Alphonse and B. Faure, "Thermal stabilization of alumina modified by lanthanum," *Microporous and Mesoporous Materials*, vol. 196, pp. 191–198, 2014.

[22] H. Firouzghalb and C. Falamaki, "Fabrication of asymmetric alumina membranes: I. Effect of SrO addition on thermal stabilization of transition aluminas," *Materials Science and Engineering B*, vol. 166, no. 2, pp. 163–169, 2010.

[23] C. Agrafiotis and A. Tsetsekou, "The effect of powder characteristics on washcoat quality. Part I: alumina washcoats," *Journal of the European Ceramic Society*, vol. 20, no. 7, pp. 815–824, 2000.

[24] C. Agrafiotis and A. Tsetsekou, "The effect of processing parameters on the properties of γ-alumina washcoats deposited on ceramic honeycombs," *Journal of Materials Science*, vol. 35, no. 4, pp. 951–960, 2000.

[25] P. Jiang, G. Lu, Y. Guo, S. Zhang, and X. Wang, "Preparation and properties of a γ-Al_2O_3 washcoat deposited on a ceramic honeycomb," *Surface and Coatings Technology*, vol. 190, no. 2-3, pp. 314–320, 2005.

[26] M. Campanati, G. Fornasari, and A. Vaccari, "Fundamentals in the preparation of heterogeneous catalysts," *Catalysis Today*, vol. 77, no. 4, pp. 299–314, 2003.

[27] M. Adamowska, O. Haddad, D. Leguillon, and P. Da Costa, "On the comprehension of mechanical, thermal and chemical evolution of exhaust gases aftertreatment catalysts," *Materials Science Forum*, vol. 783-786, pp. 1979–1985, 2014.

[28] C. Cristiani, M. Valentini, M. Merazzi, S. Neglia, and P. Forzatti, "Effect of ageing time on chemical and rheological evolution in γ-Al_2O_3 slurries for dip-coating," *Catalysis Today*, vol. 105, no. 3-4, pp. 492–498, 2005.

[29] JCPDS patterns of PdO (00-041-1107,00-043-1024).

[30] S. J. Wilson, "The dehydration of boehmite, γ-AlOOH, to γ-Al_2O_3," *Journal of Solid State Chemistry*, vol. 30, no. 2, pp. 247–255, 1979.

[31] X. Krokidis, P. Raybaud, A.-E. Gobichon, B. Rebours, P. Euzen, and H. Toulhoat, "Theoretical study of the dehydration process of boehmite to γ-alumina," *The Journal of Physical Chemistry B*, vol. 105, no. 22, pp. 5121–5130, 2001.

[32] P. de Souza Santos, A. C. V. Coelho, H. de Souza Santos, and P. K. Kiyohara, "Hydrothermal synthesis of well-crystallised boehmite crystals of various shapes," *Materials Research*, vol. 12, no. 4, pp. 437–445, 2009.

[33] A. Kalantar Neyestanaki, F. Klingstedt, T. Salmi, and D. Y. Murzin, "Deactivation of postcombustion catalysts, a review," *Fuel*, vol. 83, no. 4-5, pp. 395–408, 2004.

[34] P. Forzatti, D. Ballardini, and L. Sighicelli, "Preparation and characterization of extruded monolithic ceramic catalysts," *Catalysis Today*, vol. 41, no. 1–3, pp. 87–94, 1998.

[35] T. Defraeye, "Advanced computational modelling for drying process—a review," *Applied Energy*, vol. 131, pp. 323–344, 2014.

[36] S. J. Kowalski, K. Rajewska, and A. Rybicki, "Destruction of wet materials by drying," *Chemical Engineering Science*, vol. 55, no. 23, pp. 5755–5762, 2000.

[37] S. J. Kowalski and C. Strumłło, "Moisture transport, thermodynamics, and boundary conditions in porous materials in presence of mechanical stresses," *Chemical Engineering Science*, vol. 52, no. 7, pp. 1141–1150, 1997.